Available online at www.sciencedirect.com
SCIENCE DIRECT®
Journal of Computational Physics 200 (2004) 251–266
JOURNAL OF COMPUTATIONAL PHYSICS
www.elsevier.com/locate/jcp

Constant temperature molecular dynamics simulations of energetic particle–solid collisions: comparison of temperature control methods

Yanhong Hu, Susan B. Sinnott *

Department of Materials Science and Engineering, University of Florida, 154 Rhines Hall, P.O. Box 116400, Gainesville, FL 32611-6400, USA

Received 18 August 2003; received in revised form 3 March 2004; accepted 24 March 2004
Available online 9 June 2004

Abstract

Appropriate temperature control methods must be incorporated into simulations that maintain constant temperature. A specific role played by these methods in modeling energetic particle–solid collisions is to absorb the excess energy wave generated by the collision that, if left unchecked, propagates through the material and reflects from the system boundaries. In this study, five temperature control methods are investigated for use in molecular dynamics simulations of carbon cluster deposition on diamond surfaces. These five methods are the Nosé–Hoover thermostat, the generalized Langevin equation (GLEQ) approach, the Berendsen method, a modified GLEQ approach where an extra damping mechanism is introduced, and a combination of the GLEQ and Berendsen methods. The temperature control capability and the effectiveness of these methods at reducing the amplitude of the reflected energy wave produced in these systems are compared and discussed. It is found that the realistic performance of these methods depends on the specifics of the system, including incident energy and substrate size. Among the five methods considered, the Berendsen method is found to be effective at removing excess energy in the early stages of the deposition process, but the resultant final temperatures are relatively high in most cases. Additionally, the performance of the Nosé–Hoover thermostat is similar to that of the Berendsen method. If the diamond substrate is large enough and the incident energy is not too high, the GLEQ approach is found to be sufficient for removal of excess energy. However, the modified GLEQ approach and the new, combined thermostat perform moderately better than the other approaches at high incident energies.

AMS: 65C99; 77E05; 82A71

Keywords: Constant temperature simulations; Particle–solid collisions; Thermostat atoms; Molecular dynamics simulations

* Corresponding author. Tel.: +1-352-846-3778; fax: +1-352-846-3355.
E-mail address: ssinn@mse.ufl.edu (S.B. Sinnott).

0021-9991/$ - see front matter © 2004 Elsevier Inc. All rights reserved.
doi:10.1016/j.jcp.2004.03.019

1. Introduction

During energetic particle–solid collisions, the temperature of the substrate experiences a thermal spike when the incident particles collide with the substrate particles. The heat is then conducted away from the site of collision quickly through the substrate, causing the temperature to drop exponentially [1]. To model such processes atomistically, constant temperature molecular dynamics (MD) simulations are usually performed. Periodic boundary conditions are often used in these simulations to better mimic an infinite or semi-infinite system with a finite number of atoms [2]. Sometimes some atoms at the system boundaries are held fixed to maintain the structure of the substrate. However, these boundary conditions can result in the nonphysical reflection of energy from the boundary, which will then produce spurious effects on the simulation results. Consequently, constant temperature MD simulations make use of methods that can allow some atoms to effectively absorb the extra energy pumped into a system (including any reflected energy) and thus successfully control the system temperature in a physically reasonable manner [2].

Temperature is a thermodynamic quantity. For a system containing N particles, the temperature can be related to the average kinetic energy ($\langle K \rangle$) of the system through the principle of equipartition of energy, which states that every degree of freedom has an average energy of $k_B T/2$ associated with it [3]. That is,

$$\langle K \rangle = \left\langle \sum_i^N \frac{1}{2} m \mathbf{v}_i^2 \right\rangle = \frac{N_f k_B T}{2}, \tag{1}$$

where N_f is the number of degrees of freedom, k_B is the Boltzmann constant, and T is the thermodynamic temperature. Similarly, the instantaneous kinetic temperature can be defined as

$$T_{ins} = \frac{2K}{N_f k_B}. \tag{2}$$

The average of the instantaneous kinetic temperature of all the system particles is equal to the thermodynamic temperature of the system.

Since the temperature is related to the kinetic energy, in order to control the temperature, the velocities of the particles in the simulation system must be adjusted. One way to do this is to directly rescale the velocity of each particle, as shown in the following equation:

$$\left(\frac{\mathbf{v}_{new}}{\mathbf{v}_{old}} \right)^2 = \frac{T}{T_{ins}}, \tag{3}$$

where $\mathbf{v}_{new}$ is the rescaled velocity and $\mathbf{v}_{old}$ is the velocity before the rescaling. This method, called the velocity rescaling method, is very simple and adds (or subtracts) energy to (or from) the system efficiently. However, this direct velocity rescaling method is very coarse and far removed from the way energy is actually dissipated [2].

More sophisticated constant temperature schemes than the velocity rescaling method have been proposed. Among these schemes, the generalized Langevin equation (GLEQ) approach [4], Berendsen method [5], and Nosé–Hoover thermostat [6–8] are the three most commonly used methods and thus are considered in this study. In all these schemes, the velocities of the particles are adjusted in the various manners discussed in detail below to maintain the system temperature at a constant value.

In order to model the particle–solid collision at constant temperature, the substrate generally consists of an impact zone embedded in a thermostat zone. The atoms in the impact zone move in response to Newtonian dynamics with no constraints, while the velocities of the atoms in the thermostat zone are modified by the temperature control scheme in use. The thermostat zone not only acts as a heat reservoir, it is also used as a cushion to absorb any reflected energy waves.

In this study, stringent tests of five temperature control methods are performed in modeling energetic cluster deposition on a solid substrate. In addition to the Nosé–Hoover thermostat, the GLEQ approach and the Berendsen method, a variation of the GLEQ approach where extra damping is introduced to the atoms in the thermostat zone, and a combined thermostat of the GLEQ approach and the Berendsen method are also considered. The goal of this study is to determine the best thermostat method for use in MD simulations particularly of energetic particle–solid collisions to realistically control the system temperature and reduce the amplitude of reflected waves from the edges of the simulation unit cell.

2. Methods of interest

2.1. Nosé–Hoover thermostat

Inspired by the extended Lagrangian approach suggested by Anderson [9] in constant-pressure MD simulations, Nosé [6,7] proposed an "extended system" method to perform constant-temperature MD simulations. In his approach, Nosé introduces an additional degree of freedom s that corresponds to the heat bath and acts as a time scaling factor. Additionally, a parameter Q that could be regarded as the heat bath "mass" is also introduced. A simplified form of Nosé's method is implemented by Hoover by eliminating the time scaling factor while introducing a thermodynamic friction coefficient ζ [8]. Hoover's formulation of Nosé's method is commonly known as the Nosé–Hoover thermostat.

In this thermostat, for a system containing N atoms, the equations of motion can be written as (dots denote time derivatives):

$$\begin{aligned} \dot{\mathbf{r}}_i &= \frac{\mathbf{p}_i}{m_i}, \\ \dot{\mathbf{p}}_i &= \mathbf{F}_i - \zeta \mathbf{p}_i, \\ \dot{\zeta} &= \frac{1}{Q}\left(\sum_{i=1}^{N} \frac{p_i^2}{m_i} - N_{\mathrm{f}} k_{\mathrm{B}} T\right), \end{aligned} \tag{4}$$

where $\mathbf{r}_i$ is the position of atom i, $\mathbf{p}_i$ is the momentum, and $\mathbf{F}_i$ is the force applied to each atom. The third expression in Eq. (4) reveals the temperature control mechanism in the Nosé–Hoover thermostat. The term within the parentheses is the difference between the system instantaneous kinetic energy and the kinetic energy at the desired temperature. If the instantaneous value is higher than the desired temperature, the added friction force will increase to lower the temperature and vice versa.

The choice of the heat bath "mass" Q is arbitrary but critical to the successful performance of the thermostat. A small value of Q leads to rapid temperature fluctuation while large Q values result in inefficient sampling of phase space. Nosé [7] suggested that Q should be proportional to $N_{\mathrm{f}} k_{\mathrm{B}} T$ and should allow the added degree of freedom s to oscillate around its averaged value at a frequency of the same order as the characteristic frequency of the physical system. In this study, the value of Q is chosen to be 1.0×10^7 eV $(\mathrm{fs})^2$, which corresponds to the typical atomic vibration frequency of the order of 10^{12} Hz.

If one assumes an ergodic dynamic behavior, the Nosé–Hoover thermostat yields a well-defined canonical distribution in both momentum and coordinate space. However, for small systems or for high-frequency vibrational modes, the Nosé–Hoover thermostat may fail to generate a canonical distribution [2]. Tuckerman et al. [10] have recently discussed the inherent problems of the Nosé–Hoover thermostat. In order to fix these problems, more sophisticated algorithms based on the Nosé–Hoover thermostat have been proposed such as the "Nosé–Hoover chain" method of Martyna and co-workers [11,12]. However, if the molecular system is large enough, the movements of the atoms are sufficiently chaotic that the

performance of the Nosé–Hoover thermostat is usually satisfactory [2]. For this reason, the Nosé–Hoover thermostat is used in this study as one of the temperature control methods used to examine energetic particle–solid collisions.

2.2. Generalized Langevin equation approach

The GLEQ approach proposed by Adelman and Doll [4] was developed from the generalized Brownian motion theory. It models solid lattices at finite temperature using the methods of stochastic theory. In this approach, the molecular system of interest can be thought of as being embedded in a "solvent" that imposes the desired temperature; the molecules are regarded as solutes. The solvent affects the solute through the addition of two terms to the normal Newtonian equation of motion: one is the frictional force and the other is the random force.

The frictional force takes account of the frictional drag from the solvent as the solute moves. Since friction opposes motion, this force is usually taken to be proportional to the velocity of the particle but of opposite sign:

$$\mathbf{F}_{\text{friction}}(t) = -\beta \mathbf{v}(t). \tag{5}$$

The proportionality constant, β, is called the friction constant. Using the Debye solid model, β can be simply expressed as

$$\beta = \tfrac{1}{6}\pi\omega_{\text{D}}, \tag{6}$$

where ω_{D} is the Debye frequency, which is related to the experimentally measurable Debye temperature T_{D} by

$$\omega_{\text{D}} = \frac{k_{\text{B}} T_{\text{D}}}{\hbar}. \tag{7}$$

The random collisions between the solute and the solvent are controlled by the random force, $\mathbf{R}(t)$. This force is assumed to have no relation to the particle velocity and position, and is often taken to follow a Gaussian distribution with a zero mean and a variance σ^2 given by [13]

$$\sigma^2 = \frac{2m\beta k_{\text{B}} T}{\Delta t}, \tag{8}$$

where T is the desired temperature and Δt is the time step. The random force is balanced with the frictional force to maintain the system temperature [13]. Therefore, the equation of motion for a "solute" particle is

$$m\mathbf{a}(t) = \mathbf{F}(t) - \beta \mathbf{v}(t) + \mathbf{R}(t), \tag{9}$$

which is called the Langevin equation of motion. Following the Langevin equation of motion instead of Newton's second law, the velocity of the particle is thus gradually modified to bring its instantaneous kinetic temperature close to the desired system temperature.

In practice, other expressions for the frictional force and random force can be selected to better describe the physical condition of the system [1,14,15]. However, the expressions mentioned above are the simplest, and hence, the most computationally efficient. In simulations where the thermostat zone is far removed from the zone of interest, the results obtained using these simple expressions have proven to be reliable [13]. In this study, the GLEQ approach using the expressions described above for the frictional force and random force is thus chosen as one of the five temperature control schemes under consideration.

2.3. Berendsen method

Before the introduction of the Berendsen method, it is worthwhile to mention the Andersen method, which was proposed in 1980 [9]. This method can be thought of as a system that is coupled to a thermal bath held at the desired temperature. The coupling is simulated by random "collisions" of system particles with thermal bath particles. After each collision, the velocity of a randomly chosen system particle is reset to a new value that is randomly drawn from the Maxwell–Boltzmann distribution corresponding to the desired temperature. In practice, the frequency of random collisions is usually chosen such that the decay rate of energy fluctuations in the simulation is comparable to that in a system of the same size embedded in an infinite thermal bath. This method is simple and consistent with a canonical ensemble, but it introduces drastic change to the system dynamics [2].

A relatively gentle approach is the Berendsen method [5]. Just as in the Anderson method, the system is coupled to an imaginary external thermal bath held at a fixed temperature T. However, the exchange of thermal energy between the system and the thermal bath is much more gradual. Instead of drastically resetting the velocity of the particle to a new value, the velocity of the particle is gradually scaled by multiplying it by a factor λ given by

$$\lambda = \left[1 + \frac{\Delta t}{\tau_T}\left(\frac{T}{T_{ins}} - 1\right)\right]^{1/2}, \tag{10}$$

where Δt is the time step and τ_T is the time constant of the coupling. In this way, the velocities of the particles are adjusted such that the instantaneous kinetic temperature T_{ins} approaches the desired temperature T.

The strength of the coupling between the system and the thermal bath is controlled through the use of an appropriate coupling time constant τ_T. If rapid temperature control is desired, a small τ_T can be chosen. Consequently, the value of λ will be large and the change in the velocity will be drastic. On the other hand, if weak coupling is needed to minimize the disturbance of the system, a large value can be assigned to τ_T. In the evaluation of their own method [5], Berendsen et al. concluded that static average properties were not significantly affected by the coupling time constant, but the dynamic properties were strongly dependent on it. Their testing showed that reliable dynamic properties could be derived if τ_T was above 0.1 ps.

The Berendsen method is quite flexible in that the coupling time constant can easily be varied to suit the needs of a given application. However, the Berendsen method does have one serious problem. Although the ensemble sampled by the Berendsen method is approximately the canonical ensemble, it does not rigorously reproduce the canonical distribution [12,16]. Therefore, caution must be taken when using the Berendsen method. In this study, the ratio of $\Delta t/\tau_T$ in Eq. (10) is set to be 0.1 because it gives the best compromise between ideal temperature control and disturbance of the physical behavior of the system.

2.4. A variation of the GLEQ approach and a combined thermostat of the GLEQ and the Berendsen methods

Haberland and co-workers [17–22] performed MD simulations to study the deposition of large metal clusters on metal surfaces. They considered clusters of more than 500 metal atoms/cluster and incident energies in the keV range. Their investigation showed that the conventional GLEQ approach described in Section 2.2 was not sufficient to reduce the artificial effects caused by reflected waves from the boundaries of the simulation unit cell [17]. Therefore, they suggested a new approach to system temperature control in which the original atoms were replaced by fewer, heavier atoms [17]. This allows one to choose a large thermostat zone without losing computational efficiency. Therefore, the backscattering of the elastic wave could be sufficiently delayed. In addition, the atoms at the boundary of the impact zone and the new thermostat zone were damped relative to the motion of their neighbors. This is an efficient extra damping mechanism, especially for the high frequency part of the reflected wave [17]. However, the new thermostat

lattice should have the same elastic properties as the bulk and match the lattice structure of the impact zone. For crystalline materials that have FCC lattice structure, this is relatively easy to realize by employing a thermostat zone with a simple cubic structure and the thermostat atoms with a mass four times that of the original atoms [22]. But this approach is nontrivial to implement for materials with complex lattice structures.

Consequently, Haberland's modified GLEQ approach is presently restricted to FCC materials. In this study, a modified GLEQ approach inspired by the work of Haberland and co-workers, called the MGLEQ method, is presented. In the MGLEQ method, no replacement of thermostat atoms is introduced; this method is thus applicable to systems of any crystal structure. However, extra damping for the thermostat atoms is considered in that these atoms follow the modified Langevin equation of motion

$$m\mathbf{a}_i(t) = \mathbf{F}_i(t) - \beta[\mathbf{v}_i(t) - \overline{\mathbf{v}_{i,\mathrm{nn}}}(t)] + \mathbf{R}_i(t), \tag{11}$$

in which each thermostat atom i is further damped relative to the average velocity of its nearest neighbors $\overline{\mathbf{v}_{i,\mathrm{nn}}}$. Although this modification is slight, the performance of the MGLEQ approach is anticipated to be different from the GLEQ approach especially for deposition processes at high incident energies. This method is also rigorously tested to assess its effectiveness to both control the system temperature and reduce the amplitude of reflected energy waves.

Compared to the Berendsen method, the GLEQ approach makes more physical sense and modifies atomic velocities more gently. Nevertheless, the GLEQ approach involves the extra calculations of forces; therefore it is slightly more complicated and time-consuming than the Berendsen method. In this study, a combined thermostat scheme of the GLEQ approach and the Berendsen method (hereafter denoted as BnG) is also developed. The combination is realized by simply dividing the original thermostat zone into two smaller zones: the one that directly borders the impact zone has the GLEQ scheme applied to it, while the other has the Berendsen scheme applied to it. Testing is done to assess whether this combined method combines the advantages of these two methods.

3. Application and testing

The deposition of a single C_{20} molecule on a hydrogen-terminated diamond (1 1 1) substrate at room temperature (300 K) is considered as a test of the five thermostat schemes presented in the previous section. The initial distance between the fullerene and the substrate is around 4 Å and the C_{20} molecule is deposited along the surface normal. The substrate contains an impact zone of atoms that is 2.4 nm × 2.4 nm × 1.0 nm in size. This impact zone is embedded in a thermostat zone of atoms with four walls that are 1.0 nm thick and a bottom layer that is 1.6 nm deep, as schematically illustrated in Fig.1. The dimensions of the entire substrate are therefore 3.4 nm × 3.4 nm × 2.6 nm. The number of atoms contained in the impact zone and the thermostat zone are 1280 and 4320, respectively. Two-dimensional periodic boundary conditions are

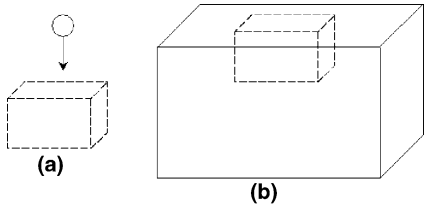

Fig. 1. The substrate layout: (a) the impact zone and (b) the impact zone embedded in the thermostat zone.

applied within the impact plane of the substrate. The bottom-most hydrogen layer is held fixed throughout the simulations to prevent translation of the substrate in space.

Various incident energies of 1, 5, 10, 20, and 40 eV/atom are considered. The third-order Nordsieck-Gear predictor–corrector algorithm is used to integrate the equations of motion [23]. The reactive empirical bond order (REBO) potential for hydrocarbons [24] coupled with long-range Lennard–Jones (LJ) potentials [2] is used to calculate the interatomic forces for the atoms in the cluster and in the impact zone. These atoms are denoted as active atoms. The velocities of the atoms in the thermostat zone are modified using one of the five temperature control schemes described in Section 2 to adjust the energy flow within the system. These atoms are therefore called thermostat atoms.

Because of the propagation of energy waves along the periodic boundaries, the substrate temperature after the deposition may not converge to 300 K, which is the desired temperature. Typically, the final temperature is higher than the desired value. But the performance of the temperature control method is assumed to be satisfactory if it brings the final temperature lower than 350 K. Of course, the closer the final temperature is to 300 K, the better the performance of the temperature control scheme.

4. Results and discussion

Deposition at 1 eV/atom (20 eV/C_{20}) is considered first. This incident energy is well below the binding energy of the carbon atoms in the C_{20}, which is approximately 5.9 eV/atom [25]. Therefore, during deposition, the original fullerene cage structure is not destroyed although deformation is observed. The degree of deformation induced by the collision varies slightly when different temperature control methods are applied to the thermostat atoms. The cluster only deforms slightly when the GLEQ and MGLEQ approaches are used, but it deforms slightly more in the cases where the Nosé–Hoover thermostat, the Berendsen method and the BnG scheme are used. In all cases, the cluster does not attach to the substrate; instead, the deformed cluster bounces back into the vacuum and gradually recovers its original spherical configuration.

A reference simulation is performed at the same incident energy of 1 eV/atom where no thermostat approach is used. Instead, all the atoms (except the bottom fixed hydrogen atoms) follow normal Newtonian dynamics. Since there is no special temperature control method used, a large substrate that is 5.2 nm $\times$ 5.2 nm $\times$ 3.1 nm is used. In this reference simulation, although there is no damage to the fullerene molecule on collision, its original cage structure deforms significantly. The whole deformed fullerene then leaves the substrate and slowly recovers its original shape. The temporal evolutions of the substrate temperature in this reference simulation and the simulations using the five temperature control methods are plotted in Fig. 2. Even though the "thermostat zone" in the reference substrate is at least three times as big as the thermostat zone used in the simulations where various temperature control methods are applied, the energy dissipation is obviously not effective in the reference substrate, as the system temperature fluctuates about 392 K. In contrast, after 3 ps, the substrate temperature is less than 320 K when various temperature control methods are employed ($\sim$320 K in the case of the Nosé–Hoover thermostat; 314 K in the cases of the GLEQ and MGLEQ approaches; 317 and 318 K when the Berendsen method and the BnG are used, respectively). This finding provides direct evidence as to why effective temperature control methods are necessary in the simulation of energetic deposition at constant temperature. Except for the fact that the substrate temperature oscillates significantly during the initial 0.45 ps when the Nosé–Hoover thermostat is used, the five temperature control methods under consideration perform almost equally well at 1 eV/atom in that the five curves essentially overlap after a relatively short amount of time, as displayed in Fig. 2.

When the deposition occurs at 5 eV/atom (1 0 0 eV/C_{20}), chemical reactions occur between the cluster and the substrate. Due to the formation of collision-induced covalent bonds, the severely deformed cluster sticks to the substrate before it recovers its cage structure during atomic relaxation. When deposition occurs

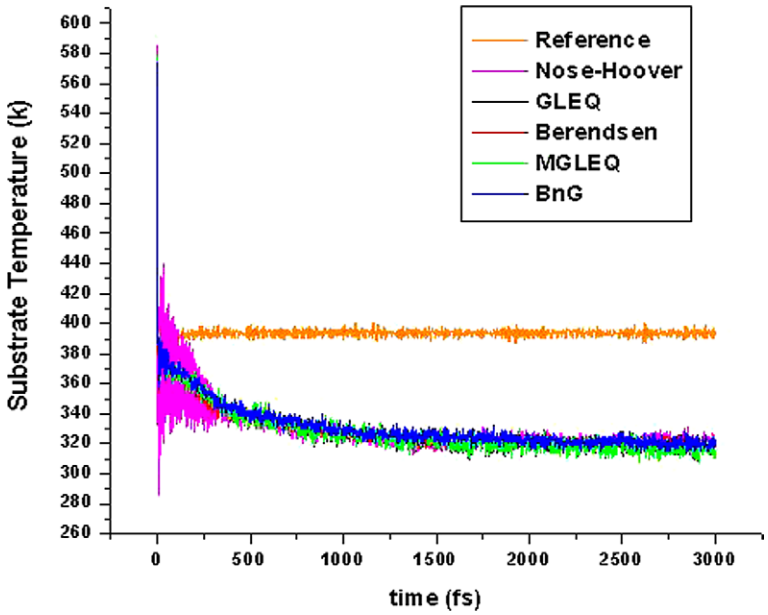

Fig. 2. The temporal evolution of the substrate temperature in a reference simulation with no temperature control method and simulations using the five temperature control methods described in the text when the C_{20} is deposited with an incident energy of 1 eV/atom.

at 10 eV/atom (200 eV/C_{20}), the cage structure of C_{20} is destroyed and the damaged cluster attaches to the substrate surface. The changes of the substrate temperature are portrayed in Figs. 3(a) and (b) for depositions at 5 and 10 eV/atom, respectively. As shown in these figures, the change of the substrate temperature during the first 1 ps varies when different temperature control methods are used. The Berendsen method reduces the temperature most dramatically at the beginning. Although the fluctuations in the substrate temperature during the initial 0.3–0.45 ps are still more obvious in the Nosé–Hoover thermostat than in the other four temperature control schemes, the amplitude of the oscillation decreases at 5 eV/atom as compared to deposition at 1 eV/atom, and decreases even more at 10 eV/atom. However, as the relaxation progresses, the behavior of the Nosé–Hoover thermostat appears very similar to that of the Berendsen method. At last, all the five curves overlap and the substrate temperature finally stabilizes at around 310–330 K.

When the deposition takes place at 20 eV/atom (400 eV/C_{20}), the cage structure of the C_{20} molecule is completely destroyed. The fragments from the cluster react with the substrate carbon atoms and nucleate a strongly adhering film. The phenomena predicted to occur in the simulations are not significantly different in the systems where different temperature control methods are used, but the difference in the substrate temperature change is much more apparent. Interestingly, the performance of the Nosé–Hoover thermostat is almost the same as the performance of the Berendsen method. As shown in Fig. 4(a), during the first 1 ps, both the Nosé–Hoover thermostat and the Berendsen method induce the most dramatic decrease in temperature, while this reduction is much gentler using the other three methods. At about 1.8 ps, the fluctuation in the temperature begins to stabilize at about 340 K in both systems using the Nosé–Hoover thermostat and the Berendsen method. However, temperature stabilization is not achieved in the systems where the other three methods are used until after 2.3 ps. The GLEQ approach appears to be the best at controlling the temperature at this incident energy because the substrate temperature after 3 ps is 327 K. In contrast, the system temperature is about 335 K using either the MGLEQ approach or the BnG method.

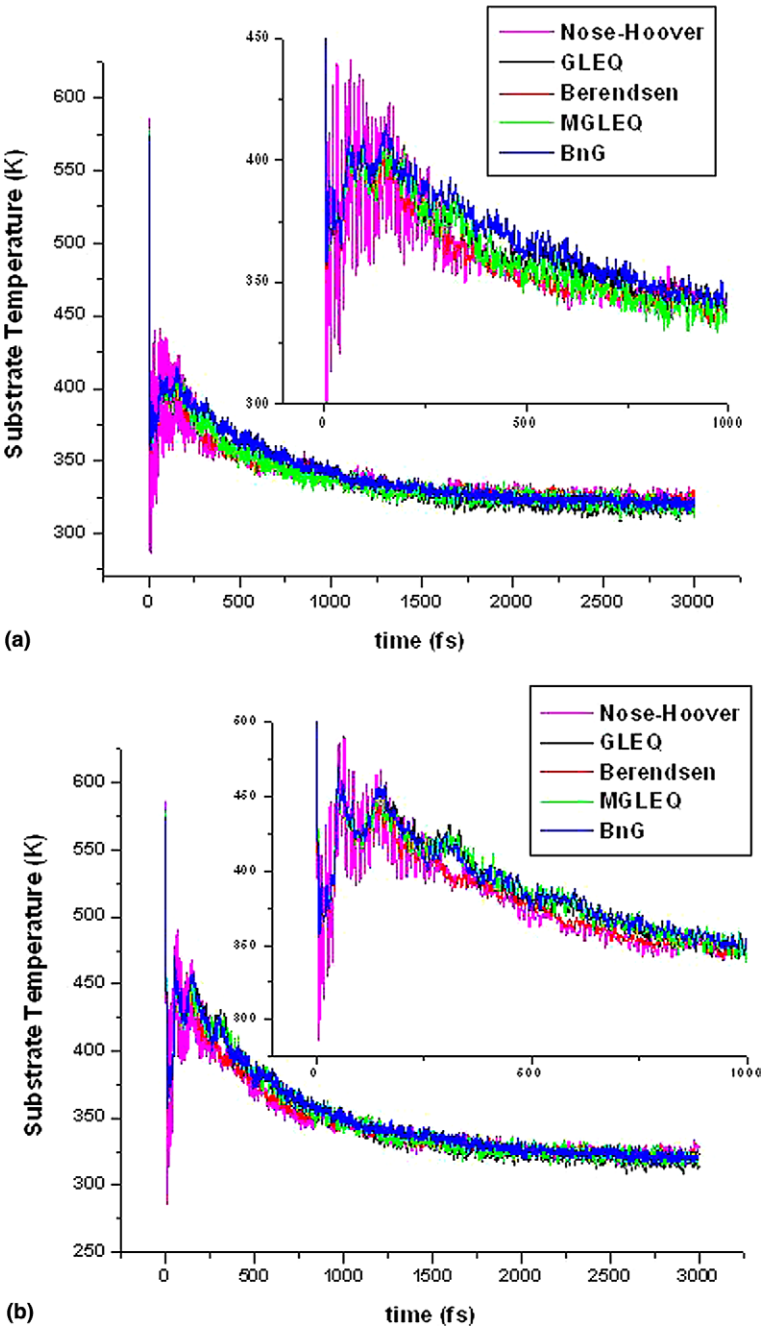

Fig. 3. The temporal evolution of the substrate temperature in the simulations using the five temperature control methods described in the text when the C_{20} is deposited with an incident energy of: (a) 5 eV/atom and (b) 10 eV/atom.

A direct way to demonstrate the energy dissipation capability of the temperature control scheme is to monitor the change of the system energy. In the deposition system considered here, the largest change in the system energy comes from the kinetic energy change because only those atoms involved in chemical

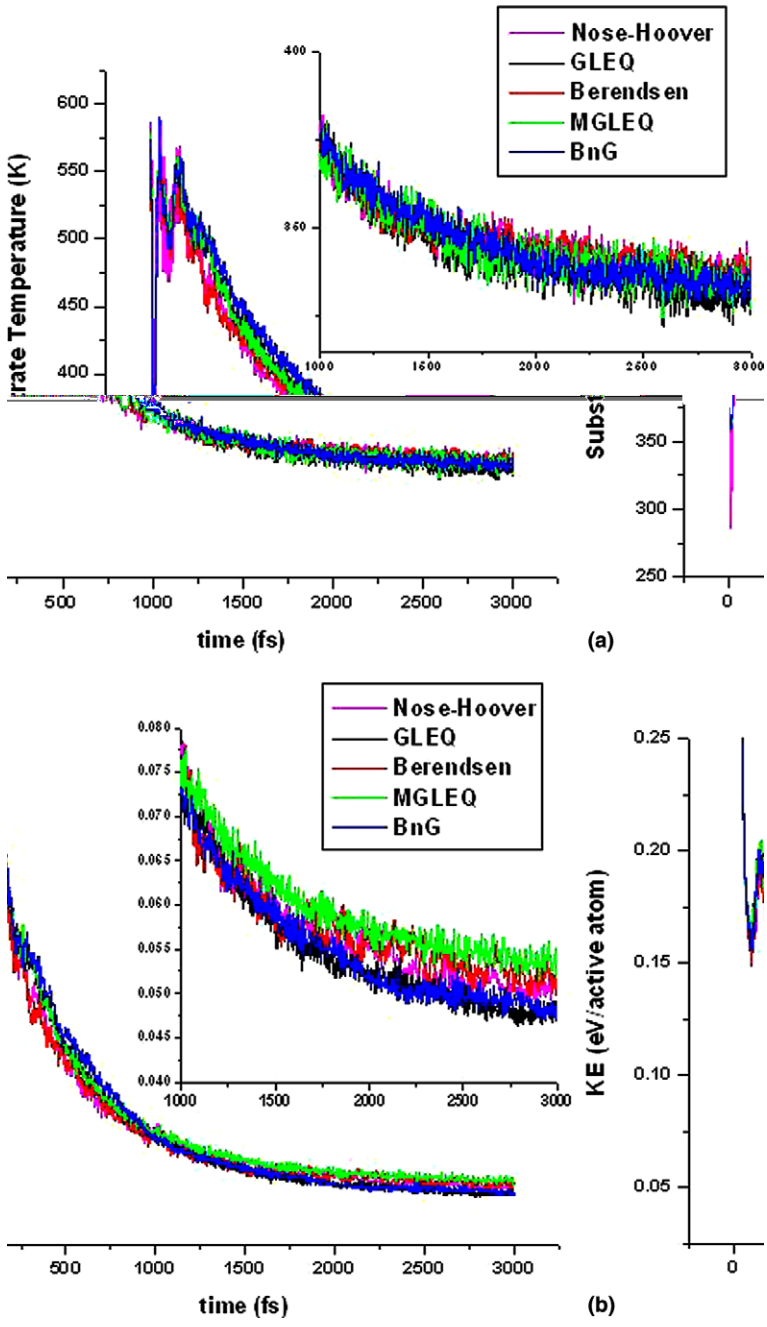

Fig. 4. The temporal evolution of: (a) the substrate temperature and (b) the kinetic energy per active atom in the simulations using the five temperature control methods described in the text when the C_{20} is deposited with an incident energy of 20 eV/atom.

reactions will have a substantial change in their potential energy, and the fraction of these atoms in the considered deposition system is very small. Therefore, the change of the kinetic energy can represent the change of the entire system energy. Fig. 4(b) gives the temporal variations of the kinetic energy per active

atom for deposition at an incident energy of 20 eV/atom. This figure better separates the curves corresponding to each temperature control method than the temporal evolution of the substrate temperature. The figure shows that before the relaxation starts (at about 1 ps), the Nosé–Hoover thermostat and the Berendsen method dissipate the extra energy most quickly, and the BnG method dissipates the energy most slowly. The curves generated from the GLEQ and MGLEQ approaches overlap at this early stage. However, at the relaxation stage, the curve of the GLEQ approach begins to separate from the curve of the MGLEQ approach. While the average kinetic energy fluctuates about 0.053 eV/atom in the Nosé–Hoover thermostat and the Berendsen method after 2 ps, this quantity continues to drop in both the GLEQ and BnG approaches. At 3 ps when the simulation stops, the GLEQ and BnG approaches have performed the best at removing the excess energy in the system.

Although the GLEQ approach is the best among the five methods for temperature control at 20 eV/atom, it becomes the worst at a high incident energy of 40 eV/atom (800 eV/C_{20}). As demonstrated in Fig. 5, both the final substrate temperature and the average kinetic energy per active atom are the highest in the system where the GLEQ approach is used. The performance of the Nosé–Hoover thermostat and the Berendsen method is not satisfactory either. In fact, the energy dissipation capability of the Nosé–Hoover thermostat is even worse than the Berendsen method, as shown in Fig. 5(b). Although at 40 eV/atom, none of the five temperature control schemes is actually good enough to bring the final substrate temperature close to the desired value, the best method at this incident energy appears to be the BnG approach that results in the lowest substrate temperature and average kinetic energy after deposition. The performance of the MGLEQ approach is next to the BnG method, which is much better than the GLEQ approach, even though only a slight modification is introduced in the MGLEQ approach as compared to the original GLEQ method.

Snapshots from the simulations at various points in time during deposition at 40 eV/atom demonstrate the different responses of the substrate when different temperature control schemes are used (Fig. 6). At 3.00 ps when the simulations stop, the substrate where the GLEQ approach is employed suffers the smallest amount of damage, while the largest amount of disorder to the substrate structure is observed in the surface where the BnG approach is used. Between approximately 0.08 and 0.24 ps, the compressed substrate moves upward. Such movements are depicted in Fig. 7 for the five substrates with different temperature control schemes applied. Although these displacement fields look quite similar, the details are different, especially the displacements of the atoms at the top right corner (see the circled areas in Fig. 7). The movement of these atoms shows the pattern of the reflected wave from the edge of the substrate when the Nosé–Hoover thermostat, the GLEQ approach, the Berendsen method, and the MGLEQ approach are used. This reflected wave could cause over-relaxation of the substrate atoms, which somewhat "heals" part of the damage to the structure. However, this pattern is not clearly present in the substrate where the BnG approach is used. In other words, the BnG approach better suppresses the amplitude of the reflected wave than the other four schemes.

In summary, at low incident energies ($\leqslant 10$ eV/atom in this study), the five temperature control methods are all sufficient to control the system temperature and delay the backscattering of the reflected wave. However, when the incident energy becomes high, variations in the performance of the five methods become apparent. These differences result from their differing abilities to absorb energetic waves propagating through the system at various frequencies. The Berendsen method reduces the energy quickly in the early stage of the process and quickly brings the system to equilibrium. Nonetheless, the Berendsen method is not as efficient at absorbing enough of the reflected energy wave when the incident energy is high, which results in a relatively high system temperature and energy when the system reaches equilibrium. Although the temperature control mechanism in the Nosé–Hoover thermostat is different from that in the Berendsen method, the performance of these two methods are similar in that the temporal evolution of the substrate temperature is essentially the same, especially during relaxation. At moderate incident energies (for example, 20 eV/atom), the GLEQ approach is still capable of dissipating the extra energy transmitted to the

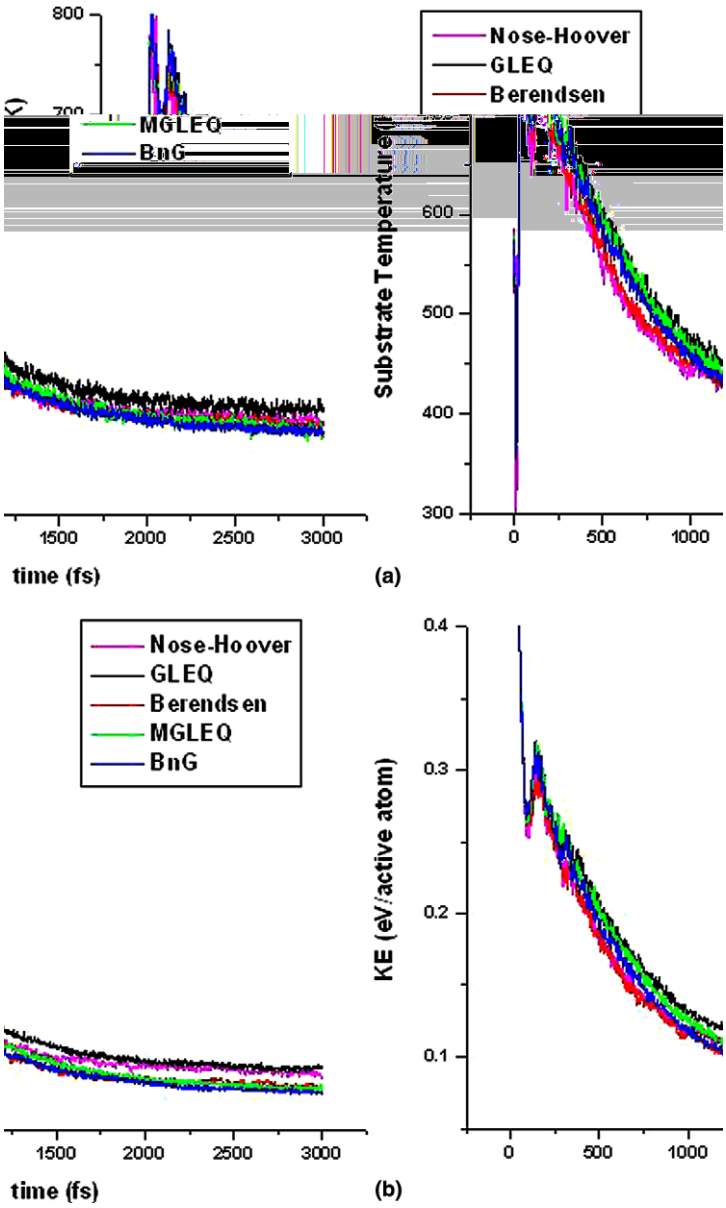

Fig. 5. The temporal evolution of: (a) the substrate temperature and (b) the kinetic energy per active atom in the simulations using the five temperature control methods described in the text when the C_{20} is deposited with an incident energy of 40 eV/atom.

surface by the cluster. Nevertheless, it fails at higher incident energy. This result is consistent with Haberland's conclusions, as mentioned in Section 2.4 [17].

The MGLEQ approach that introduces extra damping at the boundary atoms between the impact zone and the thermostat zone does indeed improve the capability of the system to control the temperature as well as absorb the reflected wave when the incident energy is high. The BnG method removes the excess energy in the most gradual manner, and this system is usually the slowest one to reach equilibrium. However, this

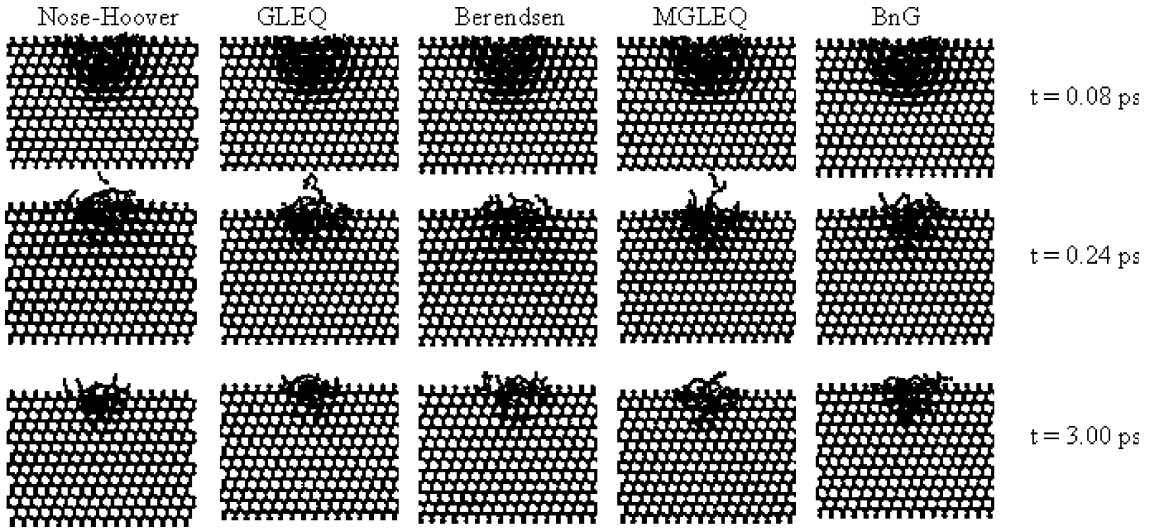

Fig. 6. Snapshots of the systems using the five temperature control methods described in the text at various moments when the C_{20} is deposited with an incident energy of 40 eV/atom.

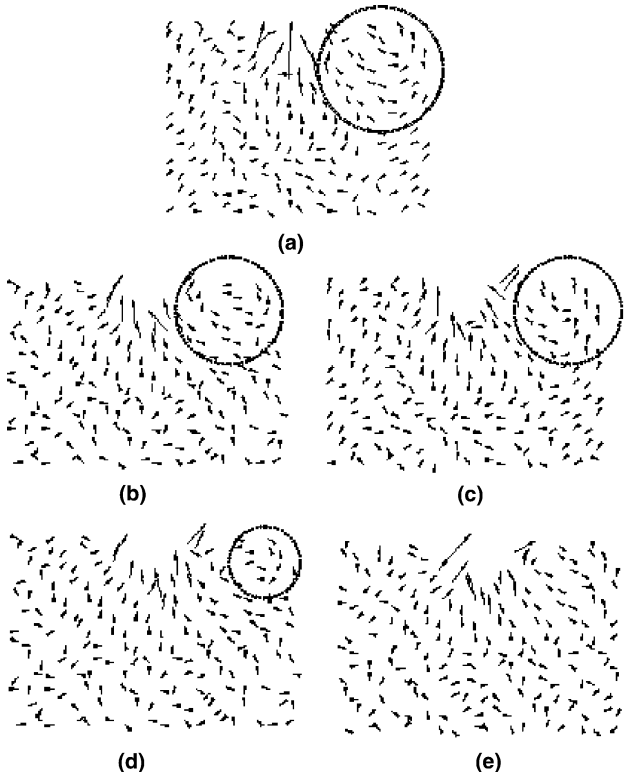

Fig. 7. The displacement fields from $t = 0.08$ to 0.24 ps in the cross-section of the (1 1 1) plane using the five temperature control methods described in the text when the C_{20} is deposited with an incident energy of 40 eV/atom: (a) Nosé–Hoover thermostat; (b) GLEQ approach, (c) Berendsen method, (d) MGLEQ approach, and (e) BnG method.

simple combination is superior to either the GLEQ approach or the Berendsen method, especially at high incident energies, if enough time is allowed for the relaxation. This can be explained as follows. The velocity adjustment algorithm in the GLEQ approach is different from that in the Berendsen method. The frequency range of the energetic wave that could be effectively absorbed by the GLEQ approach is therefore different from the Berendsen method. When the cluster collides with the substrate at a high incident energy, the

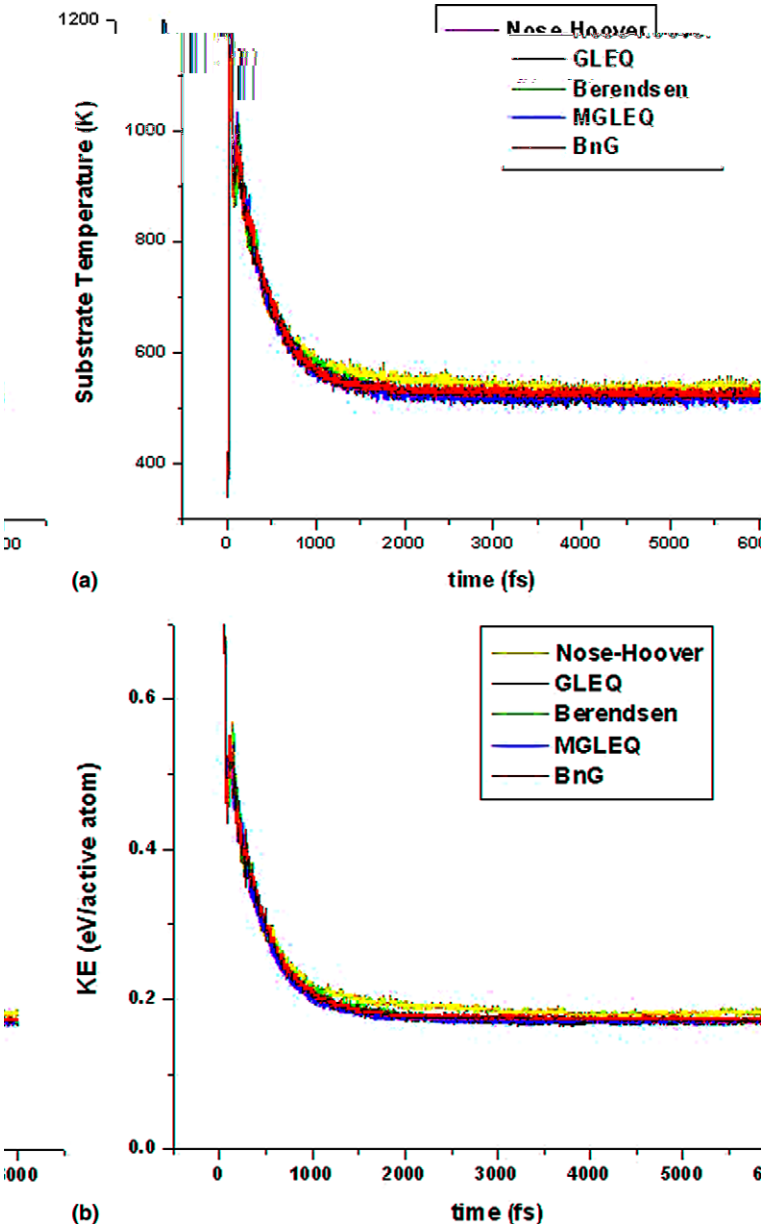

Fig. 8. The temporal evolution of: (a) the substrate temperature and (b) the kinetic energy per active atom in the deposition of C_{20} on a too-small substrate using the five temperature control methods described in the text; the C_{20} is deposited with an incident energy of 40 eV/atom.

range of the resultant energy wave frequency is wide, which may cover both the effective ranges of the GLEQ approach and the Berendsen method. Therefore, when neither the GLEQ approach nor the Berendsen method is able to completely absorb the reflected wave, their combination can do much better than either method alone.

It should be pointed out that if the substrate size is too small relative to the incident energy, none of the temperature control schemes will work well enough to remove the excess energy. This point is illustrated by a simulation of C_{20} deposition at 40 eV/atom at 300 K on a small diamond substrate with dimensions of 2.8 nm $\times$ 2.8 nm $\times$ 1.3 nm. The number of active atoms as well as the number of thermostat atoms contained in this substrate is about 1/3 of those in the substrate considered above. As given in Fig. 8(a), the Nosé–Hoover thermostat is the worst among these five schemes as the substrate temperature monitored using the Nosé–Hoover thermostat finally fluctuates at about 540 K, while the temperature is about 20 K lower when the other four schemes are used. However, both the final substrate temperature and the average kinetic energy per active atom are too high to be acceptable in each system where the five temperature control schemes are used. After 1.5 ps, the system appears to reach equilibrium and extended relaxation does not help to reduce the temperature and the energy, which indicates the reflected wave bouncing back and forth within the system.

It should be recognized that there is no real life counterpart to the thermostat atoms because of the additional constraints applied to them. The number of thermostat atoms should be large enough to bring the system temperature to the desired value. But meanwhile, in order to get reliable simulation predictions, the thermostat zone should be far away from the area where the chemical processes of interest occur. This requires the impact zone, where the atoms follow normal Newtonian dynamics, to be relatively large within the limitations of the available computer system.

5. Conclusions

In modeling energetic particle–solid collisions, the performance of the temperature control method depends on the incident energy of the particle and the substrate size. No matter which method is chosen, a large enough substrate with appropriate arrangement of the impact zone and the thermostat zone is first required.

The Berendsen method and the Nosé–Hoover thermostat are very effective at removing excess energy in the early stages of the deposition process; however, the resultant equilibrium properties are not always optimum. In modeling sputter deposition of thin films, Fang et al. [1] compared the performance of the GLEQ approach and the Nosé–Hoover thermostat. They concluded that the GLEQ approach was a better selection than the Nosé–Hoover thermostat because the GLEQ approach is a proportional control algorithm that changes the temperature exponentially as a function of the friction constant and the initial conditions, which gives a reasonable description of the deposition process. In this study, the GLEQ approach using the Debye solid model is also found to perform better than the Nosé–Hoover thermostat if the incident energy is not too high. In fact, when the deposition occurs at energy lower than 40 eV/atom, the equilibrated substrate temperature achieved using the GLEQ approach is always around 10 K lower than the temperature reached using the Nosé–Hoover thermostat. At a high incident energy, the modified GLEQ approach is better than the conventional GLEQ algorithm due to the extra damping. Not unexpectedly, the combination of the GLEQ approach and the Berendsen method is better at controlling the system temperature than either the GLEQ approach or the Berendsen method at high incident energies.

Acknowledgements

The authors gratefully acknowledge the support of the National Science Foundation through Grant CHE-0200838 and thank Inkook Jang and Ki-Ho Lee for many useful discussions.

References

[1] C.C. Fang, V. Prasad, R.V. Joshi, F. Jones, J.J. Hsieh, A process model for sputter deposition of thin films using molecular dynamics, in: S. Rossnagel (Ed.), Thin Films: Modeling of Film Deposition for Microelectronic Applications, vol. 22, Academic Press, San Diego, CA, 1996, pp. 117–173.
[2] D. Frenkel, B. Smit, Understanding Molecular Simulation: From Algorithms to Applications, Academic Press, San Diego, CA, 1996.
[3] R.T. Dehoff, Thermodynamics in Materials Science, McGraw-Hill, New York, 1993.
[4] S.A. Adelman, J.D. Doll, Generalized Langevin equation approach for atom–solid-surface scattering – general formulation for classical scattering off harmonic solids, J. Chem. Phys. 64 (1976) 2375–2388.
[5] H.J.C. Berendsen, J.P.M. Postma, W.F. Vangunsteren, A. Dinola, J.R. Haak, Molecular-dynamics with coupling to an external bath, J. Chem. Phys. 81 (1984) 3684–3690.
[6] S. Nosé, A molecular-dynamics method for simulations in the canonical ensemble, Mol. Phys. 52 (1984) 255–268.
[7] S. Nosé, A unified formulation of the constant temperature molecular-dynamics methods, J. Chem. Phys. 81 (1984) 511–519.
[8] W.G. Hoover, Canonical dynamics – equilibrium phase-space distributions, Phys. Rev. A 31 (1985) 1695–1697.
[9] H.C. Andersen, Molecular-dynamics simulations at constant pressure and/or temperature, J. Chem. Phys. 72 (1980) 2384–2393.
[10] M.E. Tuckerman, Y. Liu, G. Ciccotti, G.J. Martyna, Non-Hamiltonian molecular dynamics: generalizing Hamiltonian phase space principles to non-Hamiltonian systems, J. Chem. Phys. 115 (2001) 1678–1702.
[11] G.J. Martyna, M.L. Klein, M. Tuckerman, Nosé–Hoover chains – the canonical ensemble via continuous dynamics, J. Chem. Phys. 97 (1992) 2635–2643.
[12] D.J. Tobias, G.J. Martyna, M.L. Klein, Molecular-dynamics simulations of a protein in the canonical ensemble, J. Phys. Chem. 97 (1993) 12959–12966.
[13] B.J. Garrison, P.B.S. Kodali, D. Srivastava, Modeling of surface processes as exemplified by hydrocarbon reactions, Chem. Rev. 96 (1996) 1327–1341.
[14] B.L. Holian, R. Ravelo, Fracture simulations using large-scale molecular-dynamics, Phys. Rev. B 51 (1995) 11275–11288.
[15] W. Cai, M. de Koning, V.V. Bulatov, S. Yip, Minimizing boundary reflections in coupled-domain simulations, Phys. Rev. Lett. 85 (2000) 3213–3216.
[16] M. D'Alessandro, A. Tenenbaum, A. Amadei, Dynamical and statistical mechanical characterization of temperature coupling algorithms, J. Phys. Chem. B 106 (2002) 5050–5057.
[17] M. Moseler, J. Nordiek, H. Haberland, Reduction of the reflected pressure wave in the molecular-dynamics simulation of energetic particle–solid collisions, Phys. Rev. B 56 (1997) 15439–15445.
[18] H. Haberland, Z. Insepov, M. Karrais, M. Mall, M. Moseler, Y. Thurner, Thin-films from energetic cluster-impact – experiment and molecular-dynamics simulations, Nucl. Instrum. Methods B 80-1 (1993) 1320–1323.
[19] H. Haberland, Z. Insepov, M. Moseler, Molecular-dynamics simulation of thin-film growth by energetic cluster-impact, Phys. Rev. B 51 (1995) 11061–11067.
[20] H. Haberland, M. Moseler, Y. Qiang, O. Rattunde, T. Reiners, Y. Thurner, Energetic cluster Impact (ECI): a new method for thin-film formation, Surf. Rev. Lett. 3 (1996) 887–890.
[21] M. Moseler, J. Nordiek, O. Rattunde, H. Haberland, Simple models for film growth by energetic cluster impact, Radiat. Eff. Def. Solids 142 (1997) 39–50.
[22] M. Moseler, O. Rattunde, J. Nordiek, H. Haberland, On the origin of surface smoothing by energetic cluster impact: molecular dynamics simulation and mesoscopic modeling, Nucl. Instrum. Methods B 164 (2000) 522–536.
[23] M.P. Allen, D.J. Tildesley, Computer Simulation of Liquids, Oxford University Press, New York, 1987.
[24] D.W. Brenner, O.A. Shenderova, J.A. Harrison, S.J. Stuart, B. Ni, S.B. Sinnott, A second-generation reactive empirical bond order (REBO) potential energy expression for hydrocarbons, J. Phys. Condens. Matter. 14 (2002) 783–802.
[25] H.P. Cheng, Cluster-surface collisions: characteristics of Xe_{55}- and C_{20}-Si[1 1 1] surface bombardment, J. Chem. Phys. 111 (1999) 7583–7592.